

## Forum

### Solar Energy Conversion by Dye-Sensitized Photovoltaic Cells

Michael Grätzel\*

Laboratory for Photonics and Interfaces, Swiss Federal Institute of Technology,  
CH-1015 Lausanne, Switzerland

Received May 24, 2005

The quality of human life depends to a large degree on the availability of energy. This is threatened unless renewable energy resources can be developed in the near future. Chemistry is expected to make important contributions to identify environmentally friendly solutions of the energy problem. One attractive strategy discussed in this Forum Article is the development of solar cells that are based on the sensitization of mesoscopic oxide films by dyes or quantum dots. These systems have already reached conversion efficiencies exceeding 11%. The underlying fundamental processes of light harvesting by the sensitizer, heterogeneous electron transfer from the electronically excited chromophore into the conduction band of the semiconductor oxide, and percolative migration of the injected electrons through the mesoporous film to the collector electrode will be described below in detail. A number of research topics will also be discussed, and the examples for the first outdoor application of such solar cells will be provided.

#### Introduction

While photovoltaics has been dominated by solid-state junction devices, usually made from crystalline or amorphous silicon and profiting from the experience and material availability resulting from the semiconductor industry, there is an increasing awareness of the possible advantages of devices based on mesoscopic inorganic or organic semiconductors commonly referred to as “bulk” junctions because of their interconnected three-dimensional structure. These are formed for example from nanocrystalline inorganic oxides, ionic liquids, and organic hole conductor or conducting polymer devices,<sup>1–8</sup> which offer the prospect of very low cost fabrication without expensive and energy-intensive high-

temperature and high-vacuum processes, compatibility with flexible substrates, and a variety of presentations and appearances to facilitate market entry, both for domestic devices and in architectural or decorative applications. It is now possible to depart completely from the classical solid-state cells, which are replaced by devices based on interpenetrating network junctions. The presence of a mesoscopic junction having an interface with a huge area endows these systems with intriguing optoelectronic properties. Contrary to expectation, devices based on interpenetrating networks of mesoscopic semiconductors have shown strikingly high conversion efficiencies, which compete with those of conventional devices. The prototype of this family of devices is the dye-sensitized solar cell (DSC), invented in the author's laboratory at the Ecole Polytechnique Fédérale de Lausanne.<sup>1</sup> This accomplishes the optical absorption and charge separation processes by the association of a sensitizer as a light-absorbing material with a wide-band-gap semiconductor of mesoporous or nanocrystalline morphology.<sup>1–4</sup>

The development of these new types of solar cells is promoted by the increasing public awareness that the earth's oil reserves will run out during this century. Because the energy needs of the planet will at least double within the next 50 years, the stage is set for a major shortage of energy

\* To whom correspondence should be addressed. E-mail: michael.graetzel@epfl.ch.

- (1) O'Regan, B.; Grätzel, M. *Nature* **1991**, *355*, 737.
- (2) Grätzel, M. *Nature* **2001**, *414*, 338.
- (3) Hagfeldt, A.; Grätzel, M. *Acc. Chem. Res.* **2000**, *33*, 269.
- (4) Bach, U.; Lupo, D.; Comte, P.; Moser, J. E.; Weissörtel, F.; Salbeck, J.; Spreitzer, H.; Grätzel, M. *Nature* **1998**, *395*, 544.
- (5) Brabec, C. J.; Sariciftci, N. S. *Mater. Today* **2000**, *3*.
- (6) Halls, J. J. M.; Pickler, K.; Friend, R. H.; Morati, S. C.; Holmes, A. B. *Nature* **1995**, *376*, 498.
- (7) Tennakone, K.; Kumara, G. R.; Kottegoda, I. R.; Perera, V. S. P. *Chem. Commun.* **1999**, 15.
- (8) Sayama, K.; Suguhara, H.; Arakawa, H. *Chem. Mater.* **1998**, *10*, 3825.

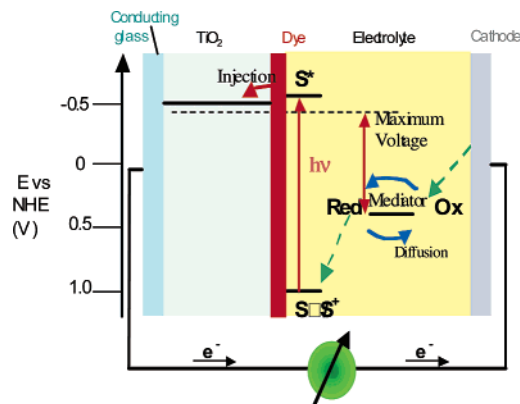


**Figure 1.** Principle of operation of the dye-sensitized nanocrystalline solar cell. Photoexcitation of the sensitizer (S) is followed by electron injection into the conduction band of a semiconductor oxide film. The dye molecule is regenerated by the redox system, which itself is regenerated at the counter electrode by electrons passed through the load. Potentials are referred to the normal hydrogen electrode (NHE). The energy levels drawn match the redox potentials of the N3 sensitizer ground state and the iodide/triiodide couple shown in Figure 5.

supply unless renewable sources can cover the substantial deficit that fossil fuels can no longer furnish.

Public concern has heightened recently because of the disastrous environmental pollution arising from all too frequent oil spills and the frightening climatic consequences of the greenhouse effect caused by the combustion of fossil fuels. Fortunately, the supply of energy from the sun to the earth is gigantic, i.e.,  $3 \times 10^{24}$  J year<sup>-1</sup> or about  $10^4$  times more than what mankind consumes currently. In other words, covering only 0.1% of the earth's surface with solar cells with an efficiency of 10% would suffice to satisfy our current needs. To tap into this huge energy reservoir of the sun remains, nevertheless, a major challenge for mankind.

The present review addresses some of the current research issues in the field of a new solar cell based on charge electron injection from molecular sensitizers or quantum dots (QDs) into a wide-band-gap semiconductor oxide of nanocrystalline morphology. We shall start with a discussion of the properties of such mesoscopic films and the principles of solar light energy harvesting and conversion to electric power accomplished by these systems.

### Operational Principle of the DSC

A schematic presentation of the operating principles of the DSC is given in Figure 1. At the heart of the system is a mesoscopic semiconductor oxide film, which is placed in contact with a redox electrolyte or an organic hole conductor. The material of choice has been TiO<sub>2</sub> (anatase), although alternative wide-band-gap oxides such as ZnO and Nb<sub>2</sub>O<sub>5</sub> have also been investigated. Attached to the surface of the nanocrystalline film is a monolayer of the sensitizer. Photoexcitation of the latter results in the injection of an electron into the conduction band of the oxide. The dye is regenerated by electron donation from the electrolyte, usually an organic solvent containing a redox system, such as the iodide/triiodide couple. The regeneration of the sensitizer by iodide intercepts the recapture of the conduction band electron by the oxidized dye. The iodide is regenerated, in turn, by the

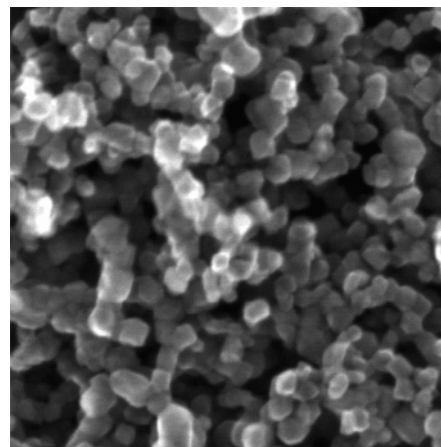


**Figure 2.** Scanning electron micrograph of a sintered mesoscopic TiO<sub>2</sub> film supported on an FTO glass. The exposed facets of the anatase nanocrystals are mainly oriented in the (101) direction. The average particle size is 20 nm.

reduction of triiodide at the counter electrode, with the circuit being completed via electron migration through the external load. The voltage generated under illumination corresponds to the difference between the Fermi level of the electron in the solid and the redox potential of the electrolyte. Overall, the device generates electric power from light without suffering any permanent chemical transformation. The first laboratory embodiment of the DSC used a titanium sheet covered with a high-surface-area “fractal” TiO<sub>2</sub> film that was produced by a sol-gel method. The roughness factor of the film was about 150. The surface of the fractal film was derivatized with the yellow ruthenium dye RuL<sub>3</sub> (L = 2,2'-bipyridyl-4,4-dicarboxylate). A cylindrical platinum wire mesh electrode served as a counter electrode. The beaker was filled with slightly acidic aqueous electrolyte containing bromide and small amounts of bromine. The open-circuit voltage of the cell was 1 V under illumination with a halogen spotlight. The device converted more than 60% of the incident photons to electric current at the absorption maximum of the sensitizer near 470 nm, and the overall conversion efficiency in full sunlight was between 1 and 2%.<sup>9</sup>

### Film Morphology and Charge-Carrier Transport

Figure 2 shows the structure of the nanocrystalline semiconductor oxide electrode used today in the DSC as an electron collector to support a molecular or QD sensitizer. The most widely used oxide material is TiO<sub>2</sub>, although other wide-band semiconductor oxides such as ZnO, SnO<sub>2</sub>, or Nb<sub>2</sub>O<sub>5</sub> have also been employed. Nanoparticles of the oxide are deposited, for example, by screen printing onto a glass or flexible plastic support covered with a transparent conducting layer of fluorine-doped tin dioxide (FTO) or tin-doped indium oxide (ITO). Each particle is coated with a monolayer of sensitizer or a QD formed by self-assembly from a staining solution.

Typically, the anatase nanoparticles are prepared with a hydrothermal method.<sup>10</sup> They exhibit predominantly a bi-

(9) Vlachopoulos, N.; Liska, P.; Augustynski, J.; Grätzel, M. *J. Am. Chem. Soc.* **1988**, *110*, 1216.

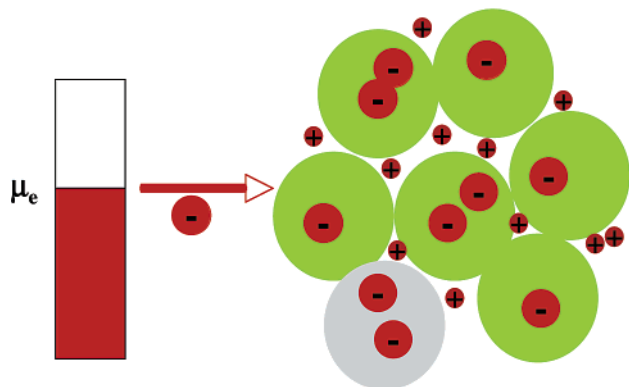


**Figure 3.** Local screening of electrons injected from a conducting support into a nanocrystalline oxide film,  $\mu_e$ , is the Fermi level of the electrons.

pyramidal shape, with the exposed facets having (101) orientation, which is the lowest energy surface of anatase. Their average size is 20 nm. A short sintering process is usually applied to ensure that the particles are electronically interconnected. To enhance the light-harvesting capacity of the dye-sensitized film in the red or near-infrared region, larger anatase particles of 200–400-nm radius are either mixed in the film or printed as an overlayer on top of the smaller particles.

These large-band-gap semiconductor oxide films are insulating in the dark; however, a single electron injected in a 20-nm-sized particle produces an electron concentration of  $2.4 \times 10^{17} \text{ cm}^{-3}$ . This corresponds to a specific conductivity of  $1.6 \times 10^{-4} \text{ S cm}^{-1}$  if a value of  $10^{-4} \text{ cm}^2 \text{ s}^{-1}$  is used for the electron diffusion coefficient.<sup>11</sup> In reality, the situation is more complex because the transport of charge carriers in these films involves trapping unless the Fermi level of the electron is so close to the conduction band that all of the traps are filled and the electrons are moving freely. Therefore, the depth of the traps that participate in the electron motion affects the value of the diffusion coefficient. This explains the observation<sup>12,13</sup> that the diffusion coefficient increases with the light intensity. Recent Monte Carlo modeling gives an excellent description of the intricacies of the electron transport in such mesoscopic semiconductor films.<sup>14</sup> Of great importance for the operation of the DSC is the fact that charges injected in the nanoparticles can be screened on the mesoscopic scale by the surrounding electrolyte, facilitating greatly electron percolation.<sup>15</sup> The electron charge is screened by the cations in the electrolyte, which eliminates the internal field, so no drift term appears in the transport equation. Figure 3 illustrates this local screening effect.

(10) Barbe, C. J.; Arendse, F.; Comte, P.; Jirousek, M.; Lenzmann, F.; Shklover, V.; Grätzel, M. *J. Am. Ceram. Soc.* **1997**, *80*, 3157.

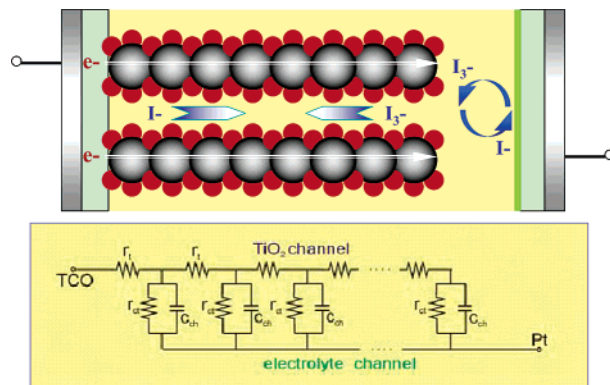
(11) Agrell, H. G.; Boschloo, G.; Hagfeldt, A. *J. Phys. Chem. B* **2004**, *108*, 12388.

(12) Cass, M. J.; Walker, A. B.; Martinez, D.; Peter, L. M. *J. Phys. Chem. B* **2005**, *109*, 5100.

(13) Frank, A. J.; Kopyidakis, N.; van de Lagemaat, J. *Coord. Chem. Rev.* **2004**, *248*, 1165.

(14) Cass, M. J.; Qiu, F. L.; Alison, W. B.; Fisher, A. C.; Peter, L. M. *J. Phys. Chem. B* **2003**, *107* (1), 113.

(15) Kubo, W.; Kitamura, T.; Hanabusa, K.; Wada, Y.; Yanagida, S. *Chem. Commun.* **2002**, 374.



**1. FT0/TiO<sub>2</sub> interface; 2. TiO<sub>2</sub>/electrolyte interface; 3. Electrolyte/Pt interface.**

**Figure 4.** Transmission line description of the conduction band electron motion through a network of mesoscopic semiconductor particles. The electrical equivalent circuit treats each particle as a resistive element. Interfacial electron transfer to the triiodide is modeled by a charge-transfer resistance connected in parallel with the capacitance of the particle/electrolyte interface. The red dots present cations from the electrolyte.

The electron motion in the conduction band of the mesoscopic oxide film is coupled with an interfacial electron-transfer reaction and with ion diffusion in the electrolyte. Bisquert<sup>16</sup> has used an infinite transmission line description to model these processes. The mesoscopic film is thought to be composed of a string of oxide nanoparticles (Figure 4). Loss of electrons to the electrolyte occurs via reduction of triiodide. The equivalent electrical circuit shown in the lower part of the figure treats each particle as a resistive element coupled to the electrolyte through the interface. The latter is presented by the electric double-layer capacitor (C) connected in parallel with the resistance (r<sub>ct</sub>) for interfacial electron transfer. The red dots denote electrolyte cations.

It is clear from Figure 4 that the movement of electrons in the conduction band of the mesoscopic films must be accompanied by the diffusion of charge-compensating cations in the electrolyte layer close to the nanoparticle surface. The cations screen the Coulomb potential of the electrons avoiding the formation of uncompensated local space charge, which would impair its motion through the film. This justifies using an “ambipolar” or effective diffusion coefficient, which contains both contributions from the electrons and charge-compensating cations<sup>17,18</sup> to describe charge transport in such mesoscopic interpenetrating network solar cells.

### Light Harvesting by Dye-Derivatized Mesoscopic Oxide Films

The absorption of light by a monolayer of dye is weak because of the fact that the area occupied by one molecule is much larger than its optical cross section for light capture. A respectable photovoltaic efficiency cannot, therefore, be obtained by use of a flat semiconductor surface but rather by use of the porous, nanostructured film of very high surface

(16) Bisquert, J. *J. Phys. Chem. B* **2002**, *106*, 325.

(17) Fabregat-Santiago, F.; Bisquert, J.; Garcia-Belmonte, G.; Boschloo, G.; Hagfeldt, A. *Sol. Energy Mater. Sol. Cells* **2005**, *87*, 117.

(18) Nakade, S.; Kubo, W.; Saito, Y.; Kanzaki, T.; Kitamura, T.; Wada, Y.; Yanagida, S. *J. Phys. Chem. B* **2003**, *107*.

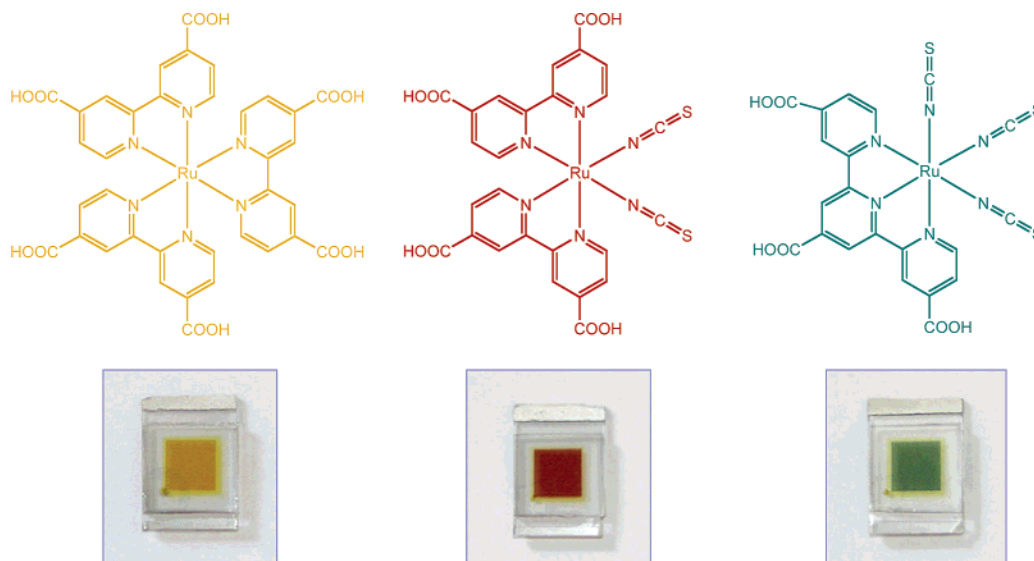


**Figure 5.** Structure of the ruthenium sensitizers  $\text{RuL}_3$  (yellow)  $\text{cis-RuL}_2(\text{NCS})_2$  (red) and  $\text{RuL}'(\text{NCS})_3$  (green) where  $\text{L} = 2,2'$ -bipyridyl-4,4'-dicarboxylic acid and  $\text{L}' = 2,2',2''$ -terpyridyl-4,4',4''-tricarboxylic acid. The lower part of the picture shows nanocrystalline  $\text{TiO}_2$  films loaded with a monolayer of the respective sensitizer. The film thickness is  $5 \mu\text{m}$ .

roughness discussed above. When light penetrates the photosensitized semiconductor “sponge”, it crosses hundreds of adsorbed dye monolayers. The mesoporous structure thus fulfills a function similar to the thylakoid vesicles in green leaves, which are stacked in order to enhance light harvesting by chlorophyll.

Apart from providing a folded surface to enhance light harvesting by the adsorbed sensitizer, the role of the nanocrystalline film is to serve as an electron conductor. The conduction band of the large-band-gap semiconductor oxide accepts the electrons from the electronically excited sensitizer. The electrons injected into the solid percolate very rapidly across the  $\text{TiO}_2$  layer. From the above-mentioned electron diffusion coefficient of  $10^{-4} \text{ cm}^2 \text{ s}^{-1}$ ,<sup>11</sup> one derives that the time required for crossing a  $\text{TiO}_2$  film, say, of  $10\text{-}\mu\text{m}$  thickness is 10 ms. During diffusion, electrons maintain their high electrochemical potential, which is equal to the quasi-Fermi level of the semiconductor under illumination. Thus, the principal function of  $\text{TiO}_2$ , apart from supporting the sensitizer, is that of charge collection and conduction. The advantage of using a semiconductor layer rather than a phospholipid membrane as in natural photosynthesis is that such an inorganic oxide is extremely stable and allows for fast electron movement. The charge transfer across the photosynthetic membrane is less rapid because it takes about  $100 \mu\text{s}$  to displace the electron across the  $50\text{-}\text{\AA}$ -thick thylakoid layer. Moreover, nature has to sacrifice more than half of the absorbed photon energy to drive the transmembrane redox processes at such a rate. In the case of the semiconductor film, the price to pay for the rapid vectorial charge displacement is small. It corresponds to at most  $50\text{--}100 \text{ meV}$  of driving force for the electron injection process at the semiconductor/sensitizer interface.

In contrast to chlorophyll, which is continuously being synthesized in the leaf, the sensitizer in the DSC must be selected to satisfy the high stability requirements encountered in practical applications. A photovoltaic device must remain

serviceable for 20 years without significant loss of performance corresponding to a number of  $50\text{--}100$  million turnovers for the dye. Recent work has focused on the molecular engineering of suitable ruthenium compounds, which are known for their excellent stability. *cis*-Di-(thiocyanato)bis(2,2'-bipyridyl)-4,4'-dicarboxylate ruthenium-(II), coded as N3 or N-719 dye depending on whether it contains four or two protons, was found to be an outstanding solar light absorber and charge-transfer sensitizer.<sup>18</sup> The performance of this red ruthenium complex was for a long time unmatched by any other dyestuff. A few years ago, a black dye was discovered that shows a performance comparable to that of N3 as a charge-transfer sensitizer in the DSC.<sup>19</sup> The structure of these sensitizers is shown in Figure 5. Recently, heteroleptic analogues to the N3 ruthenium dye carrying only one carboxylated bipyridyl ligand have been introduced, with the other bipyridyl being modified by hydrophobic chains or extended  $\pi$ -conjugated systems. These will be discussed further below.

The mesoscopic morphology of the semiconductor oxide film is essential for the efficient operation of the device. As pointed out above, on a flat surface a monolayer of dye absorbs at most a few percent of light because it occupies an area that is several hundred times larger than its optical cross section. In addition, a compact semiconductor oxide film would need to be n-doped to conduct electrons. In this case, energy-transfer quenching of the excited sensitizer by the electrons in the semiconductor would inevitably reduce the photovoltaic conversion efficiency.

Films made of oxide nanoparticles provide a strikingly simple and powerful means to achieve efficient harvesting of sunlight by the adsorbed dye monolayer.<sup>2</sup> The anatase particles shown in Figure 2 have an average size of  $20 \text{ nm}$ , and the facets exposed have mainly (101) orientation,

(19) Nazeeruddin, M. K.; Kay, A.; Rodicio, I.; Humphrey-Baker, R.; Müller, E.; Liska, P.; Vlachopoulos, N.; Grätzel, M. *J. Am. Chem. Soc.* **1993**, *115*, 6382.



corresponding to the anatase crystal planes with the lowest surface energy. Employing such oxide nanocrystals covered by a monolayer of sensitizer as light-harvesting units allowed us to overcome the notorious inefficiency problems, which had haunted all solar energy conversion devices based on the sensitization of wide-band-gap semiconductors previously.

Consider, for example, a 10- $\mu\text{m}$ -thick mesoscopic oxide film composed of 20-nm-sized particles whose real surface area is over 1000 times greater than the projected one. Because of the small size of the particle, such films show high transparency and negligible light scattering. Beer–Lambert’s law can be applied to describe the light absorption in terms of the reciprocal absorption length

$$\alpha = \sigma c \quad (1)$$

where  $\sigma$  and  $c$  are the optical absorption cross section of the sensitizer and its concentration in the mesoporous film, respectively. The value of  $\sigma$  can be derived from the decadic extinction coefficient  $\epsilon$  of the sensitizer using the relation

$$\sigma = \epsilon \times 1000 [\text{cm}^2 \text{mol}^{-1}] \quad (2)$$

Figure 5 shows the structures of three ruthenium complexes that have been widely employed as sensitizers for the DSC. The optical cross sections near the absorption maximum of these dyes are in the range of  $1 \times 10^7$ – $2 \times 10^7 \text{ cm}^2 \text{mol}^{-1}$ , and their concentration in the film at full monolayer coverage is about  $2 \times 10^{-4} \text{ mol cm}^{-3}$ . Hence,  $\alpha = (2\text{--}4) \times 10^3 \text{ cm}^{-1}$ , and the absorption length  $1/\alpha$  of these sensitizers is 2.5–5  $\mu\text{m}$ .

The light-harvesting efficiency, LHE, is derived from the reciprocal absorption length via

$$\text{LHE}(\lambda) = 1 - 10^{-\alpha d} \quad (3)$$

where  $d$  is the thickness of the nanocrystalline film. In Figure 5,  $d = 6 \mu\text{m}$ , yielding LHE values over 90% in the wavelength range near the absorption maximum of the dye. This explains the deep coloration of the nanocrystalline  $\text{TiO}_2$  layers despite of the fact that they are covered only by a monolayer of sensitizer.

The absorption length can be further reduced by exploiting light localization and optical enhancement effects. For example, incorporating 100–400-nm-sized anatase particles enhances significantly the absorption of red or near-infrared photons by the film. These light-management strategies employ scattering and photonic band-gap effects<sup>21–23</sup> to localize light in the mesoporous structure, augmenting the optical pathway significantly beyond the film thickness and

enhancing the harvesting of photons in a spectral region where the optical cross section of the sensitizer is small.

### Incident Photon to Current Conversion Efficiencies

The incident photon to current conversion efficiency (IPCE), sometimes referred to also as “external quantum efficiency” (EQE), corresponds to the number of electrons measured as photocurrent in the external circuit divided by the monochromatic photon flux that strikes the cell. This key parameter can be expressed by the product

$$\text{IPCE}(\lambda) = \text{LHE}(\lambda) \phi_{\text{inj}} \eta_{\text{coll}} \quad (4)$$

Here  $\text{LHE}(\lambda)$  is the light-harvesting efficiency for photons of wavelength  $\lambda$ ,  $\phi_{\text{inj}}$  is the quantum yield for electron injection from the excited sensitizer in the conduction band of the semiconductor oxide, and  $\eta_{\text{coll}}$  is the electron collection efficiency. Having analyzed the LHE of dye-loaded mesoscopic films above, we discuss now the other two parameters.

**(i) Dynamics of Heterogeneous Electron Injection.** The quantum yield of charge injection ( $\phi_{\text{inj}}$ ) denotes the fraction of the photons absorbed by the dye that are converted into conduction band electrons. Charge injection from the electronically excited sensitizer into the conduction band of the semiconductor is in competition with other radiative or radiationless deactivation channels. Taking the sum of the rate constants of these nonproductive channels together as  $k_{\text{deact}}$  results in

$$\phi_{\text{inj}} = k_{\text{inj}} / (k_{\text{deact}} + k_{\text{inj}}) \quad (5)$$

One should remain aware that the deactivation of the electronically excited state of the sensitizer is generally very rapid. Typical  $k_{\text{deact}}$  values lie in the range from  $10^3$  to  $10^{10} \text{ s}^{-1}$ . To achieve a good quantum yield  $\phi_{\text{inj}}$ , the rate constant for charge injection should be at least 100 times higher than  $k_{\text{deact}}$ . This means that injection rates in the picosecond range or below have to be attained. In fact, in recent years sensitizers have been developed that satisfy these requirements. These dyes should incorporate functional groups such as, for example, carboxylate, hydroxamate, or phosphonate moieties<sup>24</sup> that anchor the sensitizer to the oxide surface. Apart from forming a strong coordinative bond with the titanium surface ions, these groups also effect an enhanced electronic coupling of the sensitizer lowest unoccupied molecular orbital with the conduction band of the semiconductor. The lowest energy electronic transition for ruthenium polypyridyl complexes such as those shown in Figure 6 is of metal-to-ligand charge-transfer (MLCT) character. Thus, upon excitation the electron density shifts from the ruthenium metal to the ligand, which should be the one that carries the attaching groups and the one from which very rapid electron injection into the semiconductor takes place. With molecularly engineered sensitizers such as these, the injection times are in the pico- or femtosecond range<sup>25–28</sup> and the quantum yield of charge injection generally exceeds 90%. In fact, for

(20) Nazeeruddin, M. K.; Pechy, P.; Renouard, T.; Zakeeruddin, S. M.; Humphry-Baker, R.; Comte, P.; Liska, P.; Cevey, L.; Costa, E.; Shklover, V.; Spiccia, L.; Deacon, G. B.; Bignozzi, C. A.; Grätzel, M. *J. Am. Chem. Soc.* **2001**, *123*, 1613.

(21) Nishimura, S.; Abrams, N.; Lewis, B.; Halaoui, L. I.; Mallouk, Th. E.; Benkstein, K. D.; van de Lagemaat, J.; Frank, A. J. *J. Am. Chem. Soc.* **2003**, *125*, 6306.

(22) Halaoui, L. I.; Abrams, N. M.; Mallouk, T. E. *J. Phys. Chem.* **2005**, *109*, 6334.

(23) Hore, S.; Nitz, P.; Vetter, C.; Prahl, C.; Niggemann, M.; Kern, R. *Chem. Commun.* **2005**, *15*, 2011.

(24) Greijer, Agrell, R.; Lindgren, J.; Hagfeldt, A. *Photochem. Photobiol. A* **2004**, *164*, 23.

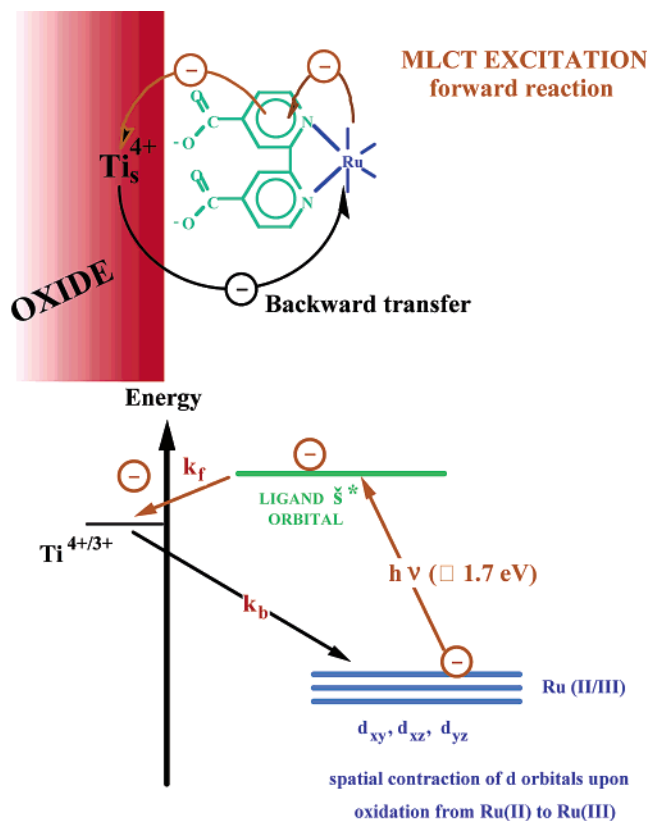


**Figure 6.** Interfacial electron transfer involving a ruthenium complex bound to the surface of  $\text{TiO}_2$  via a carboxylated bipyridyl ligand. Orbital diagram for the forward electron injection (rate constant  $k_f$ ) from the  $\pi^*$  orbital of the bipyridyl ligand into the empty  $t_{2g}$  orbitals forming the  $\text{TiO}_2$  conduction band and the backward electron transfer from the conduction band of the oxide into the  $\text{Ru(III)}$  d orbitals.

several sensitizers the electron transfer into the conduction band of the oxide is so rapid that it occurs from vibrationally hot excited states.<sup>26–28</sup>

Shown in Figure 7 is the transient absorption signal following femtosecond laser excitation of N-719 dye adsorbed on the surface of nanocrystalline titania.<sup>29</sup> The formation of the oxidized sensitizer and conduction band electrons due to heterogeneous charge transfer from the excited ruthenium complex into the conduction band of the oxide is resolved on a femtosecond time scale. Figure 7 indicates that the reaction is completed within the femtosecond laser excitation pulse. Fitted data provide a cross-correlation time of 57 fs that is consistent with the instrument response measured by Kerr gating in a thin glass window. This temporal resolution does not allow the determination of the rate of the injection process accurately, but its time

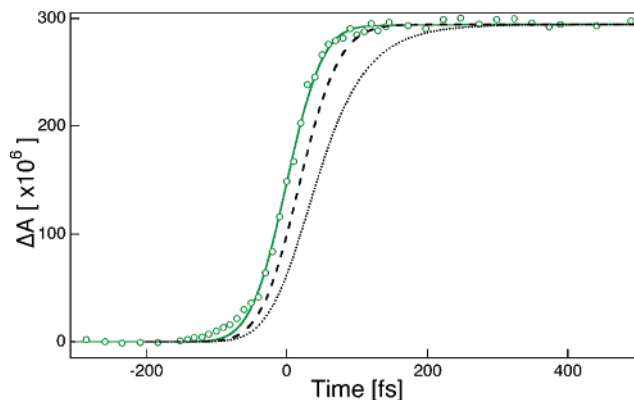


**Figure 7.** Transient absorption signal for N-719 adsorbed on nanocrystalline titania ( $\circ$ ) (pump wavelength 535 nm; probe 860 nm). The fitted instrument response is 57 fs ( $-$ ). The simulated exponential rises with time constants of 20 fs ( $- -$ ) and 50 fs ( $\cdots$ ) and convoluted with the same instrument response are shown.

constant can be estimated as being definitely shorter than 20 fs, corresponding to a rate constant  $k_{inj} > 5 \times 10^{13} \text{ s}^{-1}$ . An electron-transfer process with such a high rate can be rationalized in terms of a strong electronic coupling and of the large density of acceptor states in the semiconductor. Because nuclear motion in the molecule and its environment takes place within a time frame of at least 20 fs, the observed charge injection dynamics is certainly beyond the scope of vibration-mediated electron-transfer models.<sup>30</sup> The process rate is, therefore, likely to be limited only by the electron dephasing in the solid. Interestingly, much slower injection kinetics extending into the picosecond time domain were observed when N-719 was present in an aggregated form at the surface of the titania films.<sup>29</sup>

**(ii) Light-Induced Charge Separation.** As the next step of the conversion of light into electrical current, a complete charge separation must be achieved. On thermodynamic grounds, the preferred process for the electron injected into the conduction band of the titanium dioxide films is the back reaction with the oxidized sensitizer. Naturally, this reaction is undesirable because, instead of electrical current, it merely generates heat. For the characterization of the recombination rate, an important kinetic parameter is the rate constant  $k_b$ . It is of great interest to develop sensitizer systems for which the value of  $k_{inj}$  is high and that of  $k_b$  low.

It was shown above that, for the N-719 ruthenium sensitizer, the forward injection is an extremely rapid process occurring in the femtosecond time domain. By contrast, the back reaction of the electrons with the oxidized ruthenium complex involves a d orbital localized on the ruthenium metal whose electronic overlap with the  $\text{TiO}_2$  conduction band is small and is further reduced by the spatial contraction of the wave function upon oxidation of  $\text{Ru(II)}$  to  $\text{Ru(III)}$ . Thus, the electronic coupling element for the back reaction is 1–2 orders of magnitude smaller for the back electron transfer as compared to injection reducing the back reaction rate by the same factor.

(25) Tachibana, Y.; Moser, J. E.; Grätzel, M.; Klug, D. R.; Durrant, J. R. *J. Phys. Chem.* **1996**, *100*, 20056.

(26) Moser, J. E.; Grätzel, M. *Chimia* **1998**, *52*, 160.

(27) (a) Benkö, G.; Kallioinen, J.; Korppi-Tommola, J. E. I.; Yartsev, A. P.; Sundström, V. *J. Am. Chem. Soc.* **2002**, *124*, 489. (b) Kallioinen, J.; Benkö, G.; Sundström, V.; Korppi-Tommola, J. E. I.; Yartsev, A. P. *J. Phys. Chem. B* **2002**, *106*, 4396. (c) Benkö, G.; Kallioinen, J.; Myllyperkiö, P.; Trif, F.; Korppi-Tommola, J. E. I.; Yartsev, A. P.; Sundström, V. *J. Phys. Chem. B* **2004**, *108*, 2862.

(28) Schwarzburg, K.; Ernstorfer, R.; Felber, S.; Willig, F. *Coord. Chem. Rev.* **2004**, *248* (13–14), 1259.

(29) Wenger, B.; Grätzel, M.; Moser, J. E. *J. Am. Chem. Soc.* **2005**, in press.

(30) (a) Lanzafame, J. M.; Miller, R. J. D.; Muentner, A. A.; Parkinson, B. A. *J. Phys. Chem.* **1992**, *96*, 2820. (b) Huber, R.; Moser, J. E.; Grätzel, M.; Wachtveitl, J. *Proc. SPIE* **2003**, *5223*, 121.

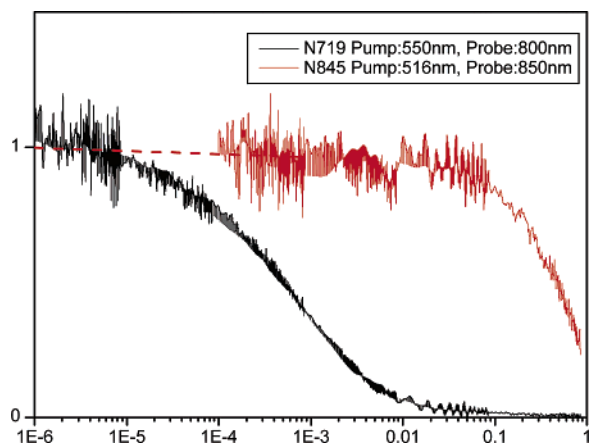


**Figure 8.** Laser photolysis of N-719 and N-845 ruthenium dyes adsorbed on nanocrystalline titania particles. The normalized transient absorption indicates the temporal decay of the oxidized N-719 (black) and N-845 (red) sensitizer due to recombination with conduction band electrons. The abscissa expresses time in units of seconds.

A second very important contribution to the kinetic retardation of charge recombination arises from the fact that this process is characterized by a large driving force and small reorganization energy, with the respective values for N-719 being 1.5 and 0.3 eV, respectively. This places the electron recapture clearly in the inverted Marcus region, reducing its rate by several orders of magnitude. This provides also a rationale for the observation that this interfacial redox process is almost independent of temperature and is surprisingly insensitive to the ambient that is in contact with the film.<sup>31</sup>

Charge recombination is, furthermore, inhibited by the existence of an electric field at the surface of the titanium dioxide film. While there is practically no depletion layer within the oxide due to the small size of the particles and their low doping level, a surface field is established spontaneously by proton transfer from the carboxylic acid groups of the ruthenium complex to the oxide surface, producing a charged dipole layer. If the film is placed in contact with a protic solvent, the latter can also act as a proton donor. In aprotic media,  $\text{Li}^+$  or  $\text{Mg}^{2+}$  are potential determining ions for  $\text{TiO}_2$ <sup>32</sup> and they may be used to charge the surface positively. The local potential gradient from the negatively charged sensitizer to the positively charged oxide drives the injection in the desired direction. The same field also inhibits the electrons from exiting the solid after injection has taken place.

Finally, the back-reaction dynamics are strongly influenced by the trapping of the conduction band in the mesoscopic film. If the diffusion of trapped electrons to the particle surface is rate-determining, the time law for the back reaction is a stretched exponential.<sup>33</sup> If, by contrast, the interfacial back electron transfer is so slow that it becomes rate-determining, then the back reaction follows first-order kinetics.

Shown in Figure 8 are results from laser photolysis experiments<sup>34</sup> that illustrate these two cases. The decay of

the transient absorption reflects the recombination of electrons from the conduction band of the titania nanoparticles with the oxidized form of the ruthenium sensitizers N-719 and N-845. In the case of N-719, interfacial recombination is faster than the electron diffusion from the interior of the particles to the surface.

Therefore, the time law for the back reaction is a stretched exponential (black curve in Figure 8). The N-845 sensitizer shown in Figure 9 has a hole-trapping triarylamine function attached to one of its bipyridyl ligands. Following electron injection, the positive charge is transferred from the ruthenium ion to the triarylamine group, moving the hole away from the surface. The increased distance retards the back electron transfer to such an extent that it becomes the rate-limiting step. Hence, a simple exponential decay is observed on a very slow time scale reaching hundreds of milliseconds.

**(iii) Charge-Carrier Collection.** The question of charge-carrier percolation over the mesoscopic particle network has already been addressed above. This important process leading to nearly quantitative collection of electrons injected by the sensitizer is presently attracting a great deal of attention. For example, impedance spectroscopy gives useful clues to rationalize the intriguing findings made with these films under band-gap illumination.<sup>35</sup>

Apart from recapture by the oxidized dye, the electrons can be lost to the electrolyte by reaction with the oxidized sensitizer from of the redox mediator, e.g., triiodide ions:

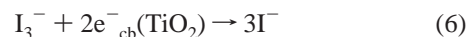
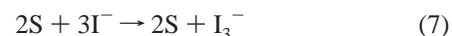


Figure 10 illustrates the injection and recombination processes. Mastering the interface to impair the unwanted back reaction remains a key target of current research.<sup>36</sup>

The efficient interception of recombination by the electron donor, e.g., iodide,



is crucial for obtaining good collection yields and a high cycle life of the sensitizer. In the case of N-719 or its amphiphilic analogue Z-907, time-resolved laser experiments have shown the interception to take place with a rate constant of about  $10^5$ – $10^7$   $\text{s}^{-1}$  at the iodide concentrations that are typically applied in the solar cell.<sup>37</sup> This is more than 100 times faster than the recombination rate and  $>10^8$  times faster than the intrinsic lifetime of the oxidized sensitizer in the electrolyte in the absence of iodide.<sup>37</sup> Cyclic voltammetry experiments carried out with solutions of I have shown its intrinsic lifetime in the oxidized state to be limited to a few seconds by intramolecular charge transfer from Ru(III) to

(33) Nelson, J.; Chandler, R. E. *Coord. Chem. Rev.* **2004**, *248*, 1181.

(34) Hirata, N.; Lagref, J.-J.; Palomares, E. J.; Durrant, J. R.; Nazeeruddin, M. K.; Grätzel, M.; Di Censo, D. *Chem. Eur. J.* **2004**, *10*, 595.

(35) Fabregat-Santiago, F.; Bisquert, J.; Garcia-Belmonte, G.; Boschloo, G.; Hagfeldt, A. *Sol. Energy Mater. Sol. Cells* **2005**, *87*, 117.

(36) Wang, P.; Zakeeruddin, S. M.; Moser, J. E.; Humphry-Baker, R.; Comte, P.; Aranyos, V.; Hagfeldt, A.; Nazeeruddin, M. K.; Grätzel, M. *Adv. Mater.* **2004**, *16*, 1806.

(37) Wang, P.; Wenger, B.; Humphry-Baker, R.; Moser, J.-E.; Teuscher, J.; Kanteleiner, W.; Mezger, J.; Stoyanov, E. V.; Zakeeruddin, S.-M.; Grätzel, M. *J. Am. Chem. Soc.* **2005**, *127*, 18.

(31) Moser, J. E.; Grätzel, M. *Chem. Phys.* **1993**, *176*, 493.

(32) Redmond, G.; Fitzmaurice, D. *J. Phys. Chem.* **1993**, *97*, 11081.



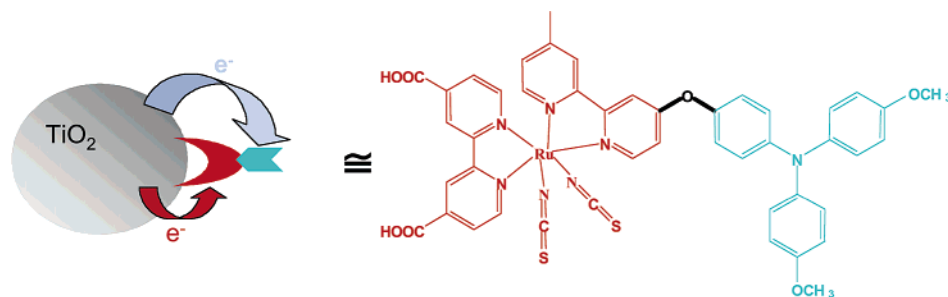


**Figure 9.** Structure of the N-845 dye and the redox processes that follow light-induced electron injection from this sensitizer into the conduction band of a titania particle.

the  $\text{SCN}^-$  group, followed by irreversible oxidation of the latter ligand. The factor of  $10^8$  explains the fact that this sensitizer can sustain 100 million turnovers in continuous solar cell operation without loss of performance.

To reach a high conversion efficiency, provisions must be made to collect all photogenerated charge carriers. IPCEs, referred to also as EQEs, should be close to unity over the near-UV, visible, and near-IR wavelength domain. A key parameter is the electron diffusion length

$$L_n = \sqrt{D_e \tau_r} \quad (8)$$

where  $D_e$  and  $\tau_r$  are the diffusion coefficient and lifetime of the electron, respectively. Quantitative collection of charge carriers can be achieved only if the electron diffusion length is greater than the film thickness ( $d$ ):

$$L_n > d \quad (9)$$

The film, in turn, needs to be significantly thicker than the light absorption length ( $1/\alpha$ ) in order to ascertain nearly quantitative harvesting of the light in the spectral absorption range of the QD or the molecular sensitizer:

$$d > 1/\alpha \quad (10)$$

The thickness of the nanocrystalline layer required to satisfy the last conditions is typically on the order of a few microns depending on the optical cross section of the sensitizer or QD and their concentration in the film as discussed above.

### QD Sensitizers

Semiconductor QDs can replace dyes as light-harvesting units in the DSC.<sup>38,39</sup> Light absorption produces excitons or electron–hole pairs in the QD. The electron is subsequently injected in the semiconductor oxide support, while the hole is transferred to a hole conductor or an electrolyte present in the pores of the nanocrystalline oxide film. Efficient and rapid hole injection from PbS QDs into triarylamine hole conductors has already been demonstrated, and IPCE values exceeding 50% have been reached without attempting to optimize the collector structure and retard interfacial electron–hole recombination.<sup>38</sup> QDs have much higher optical cross sections than molecular sensitizers, depending on their

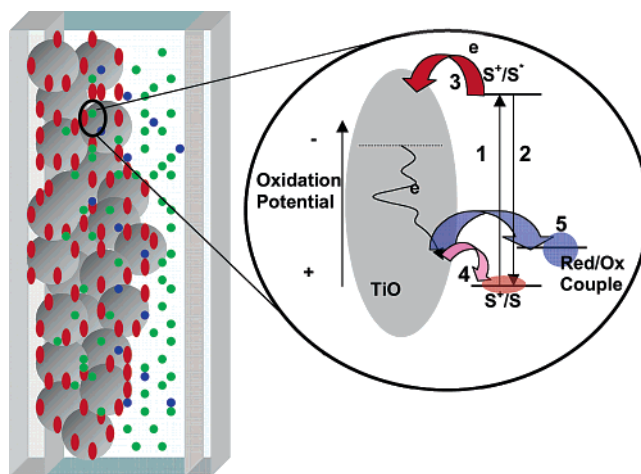


**Figure 10.** Photoinduced processes occurring during photovoltaic energy conversion at the surface of the nanocrystalline titania films: (1) sensitizer (S) excitation by light; (2) radiative and nonradiative deactivation of the sensitizer; (3) electron injection in the conduction band, followed by electron trapping and diffusion to the particle surface; (4) recapture of the conduction band electron by the oxidized sensitizer ( $\text{S}^+$ ); (5) recapture of the conduction band electrons by the oxidized form of the redox couple regenerating the sensitizer and transporting the positive charge to the counter electrode. Gray spheres: titania nanoparticles. Red dots: sensitizer. Green and blue dots: oxidized and reduced forms of the redox couple.

size. However, they also occupy a larger area on the surface of the mesoporous electrode, decreasing the QD concentration in the film. As a result, the value of the absorption length is similar to that observed for the dye-loaded films.

A very recent exciting discovery shows that multiple excitons can be produced from the absorption of a single photon by a QD via impact ionization if the photon energy is 3 times higher than its band gap.<sup>40</sup> The challenge is now to find ways to collect the excitons before they recombine. Because recombination occurs on a femtosecond time scale, the use of mesoporous oxide collector electrodes to remove the electrons presents a promising strategy, opening up research avenues that ultimately may lead to photoconverters reaching IPCE values of over 100%.

### Present Embodiments of the DSC

The most widely used sensitizer for the DSC has been *cis*- $\text{Ru}(\text{SCN})_2\text{L}_2$  ( $\text{L} = 2,2'$ -bipyridyl-4,4'-dicarboxylate), abbreviated as N3.<sup>19</sup> The redox system employed to regenerate the dye and transport the positive charges to the counter electrode has been the iodide/triiodide couple dissolved in

(38) Plass, R.; Pelet, S.; Krüger, J.; Grätzel, M.; Bach, U. *J. Phys. Chem. B* **2002**, *106*, 7578–7580.

(39) Nozik, A. J. Quantum dot solar cells. *Next Gener. Photovoltaics* **2004**, *196*.

(40) Schaller, R.; Klimov, V. I. *Phys. Rev. Lett.* **2004**, *92*, 186601.



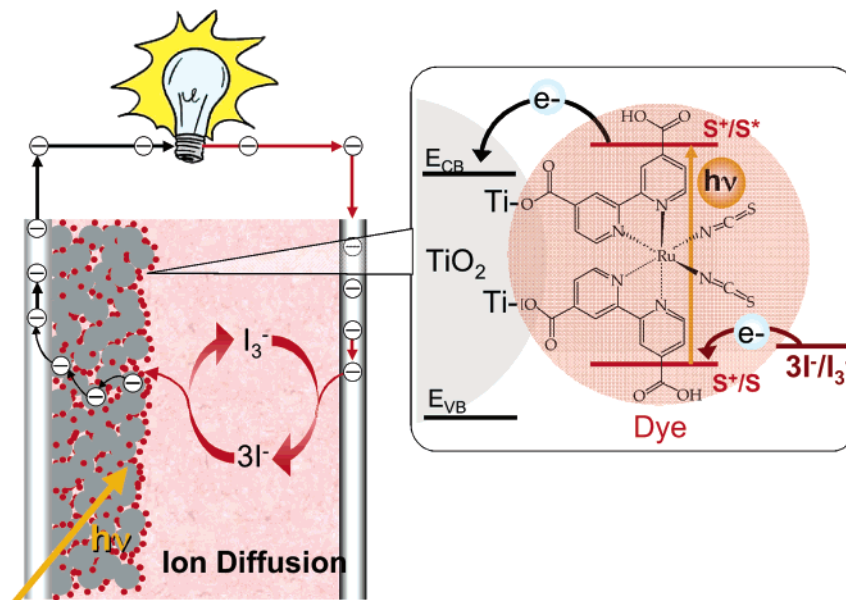


**Figure 11.** Schematic drawing showing the currently used embodiment of the DSC. It employs dye-derivatized TiO<sub>2</sub> nanocrystals as light-harvesting units. The sensitizer is *cis*-Ru(SCN)<sub>2</sub>L<sub>2</sub> (L = 2,2'-bipyridyl-4,4'-dicarboxylate). The redox system employed to regenerate the dye and transport the positive charges to the counter electrode is the iodide/triiodide couple dissolved in an organic electrolyte or in a room-temperature ionic liquid.

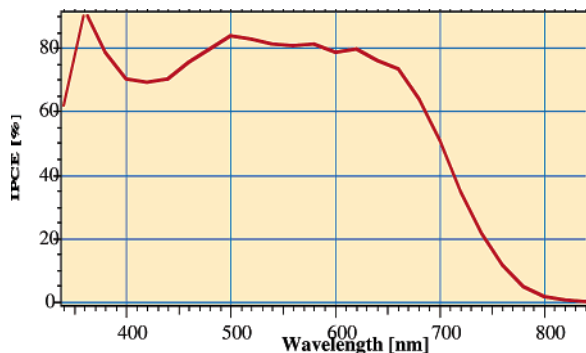


**Figure 12.** Conversion of light to electric current by mesoscopic solar cells sensitized with the ruthenium dye N-719. The IPCE is plotted as a function of the excitation wavelength. The electrolyte contains alkyl-imidazolium iodide and triiodide as the redox system.

an organic electrolyte or in a room-temperature ionic liquid, although very promising results have been obtained also with cobalt(II) complexes Figure 11 shows an operational diagram of the cell using these constituents, which form the main embodiment of the DSC to date.

### Photovoltaic Performance

The astounding performance of mesoscopic semiconductor junctions is illustrated in Figure 12, where we show the photoresponse of a state-of-the-art nanocrystalline titania film sensitized by the N-719 dye. The IPCE is plotted as a function of the wavelength. The IPCE values exceed 80% in the wavelength range near the absorption maximum of the sensitizer, which is located around 530 nm. Taking into account the light losses from the absorption and reflection by the FTO glass, the conversion of photons that strike the TiO<sub>2</sub> film into electric current is almost quantitative. Even at 700 nm, where the absorption of light by the dye is weak, as shown in Figure 13, the IPCE value is still about 50%. The titania film in Figure 12 contained 400-nm-sized light-

scattering particles, which enhance the optical path length and harvesting of light in the red wavelength region. This striking performance defies expectations because such large-area junctions should fare poorly in photovoltaic energy conversion in the presence of defects at the disordered surface, enhancing the recombination of photogenerated charge carriers.

Very high IPCEs can also be achieved with organic dyes. Such sensitizers that come close to matching the efficiency of the N-719 dye have recently been developed in Japan.<sup>42,43</sup>

These extraordinary findings are due to the specific kinetic features of the interfacial charge-transfer processes summarized in Figure 14. As discussed above, the initial events of electron injection and dye regeneration leading to photoinduced charge separation occur on a femto- to nanosecond or microsecond time scale,<sup>44</sup> while the redox capture of the electron by the oxidized relay and the electron migration across the nanocrystalline film take place within milliseconds or even seconds. The square root of the product of the electron lifetime and diffusion coefficient corresponds to the diffusion length of the electron. If the latter is greater than the film thickness, all of the photogenerated carriers will be collected.

The overall conversion efficiency of the dye-sensitized cell is determined by the photocurrent density measured at short circuit ( $I_{sc}$ ), the open-circuit photovoltage ( $V_{oc}$ ), the fill factor of the cell (ff), and the intensity of the incident light ( $I_s$ ).

$$\eta_{\text{global}} = i_{\text{ph}} V_{\text{oc}} (\text{ff}) / I_s \quad (11)$$

Under full sunlight (air mass 1.5 global, intensity  $I_s = 1000 \text{ W cm}^{-2}$ ), short-circuit photocurrents ranging from 16

- (41) Nusbaumer, H.; Zakeeruddin, S.-M.; Moser, J.-E.; Grätzel, M. *Chem-Eur. J.* **2003**, *9*, 3756.  
 (42) Hara, K.; Kurashige, M.; Dan-oh, Y.; Kasasa, C.; Ohga, Y.; Shinpo, A.; Suga, S.; Sayama, K.; Arakawa, H. *New J. Chem.* **2003**, *27*, 783.  
 (43) Horiuchi, T.; Miuraa, H.; Satoshi; Uchida Miura; et al. *Chem. Commun.* **2003**, 3036.

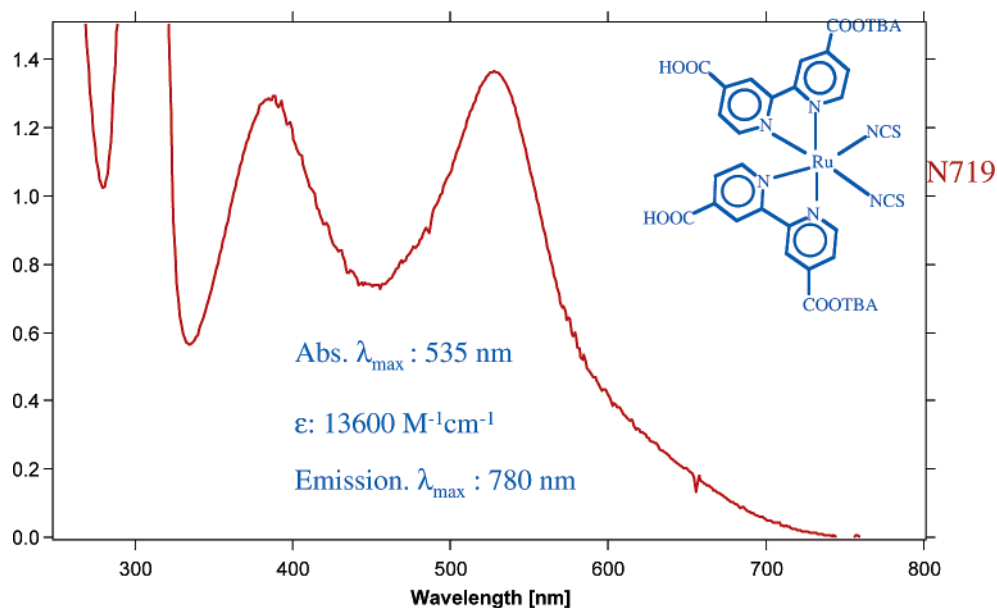


Figure 13. Absorption spectrum of the N-719 dye in ethanol featuring two MLCT bands.

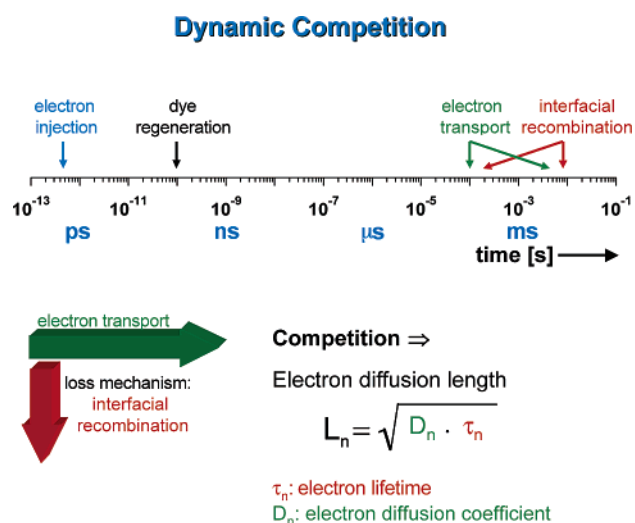


Figure 14. Dynamics of redox processes involved in the conversion of light to electric power by DSCs.

to 22 mA cm<sup>-2</sup> are reached with state-of-the-art ruthenium sensitizers, while  $V_{oc}$  is 0.7–0.86 V and ff values are 0.65–0.8. A certified overall power conversion efficiency of 10.4% was attained<sup>20</sup> in 2001. A new record efficiency of over 11% was achieved recently, and Figure 15 shows current voltage curves obtained with this cell.

While such efficiency figures render dye-sensitized cells competitive with the conventional solar devices, a commercially even more significant parameter is the dye lifetime achieved under working conditions. A recent stability test during 12 000 h of continuous full-intensity light exposure has confirmed that this system does not exhibit any inherent instability,<sup>46</sup> in contrast to amorphous silicon, which because of the Stabler–Wronski effect undergoes photodegradation.

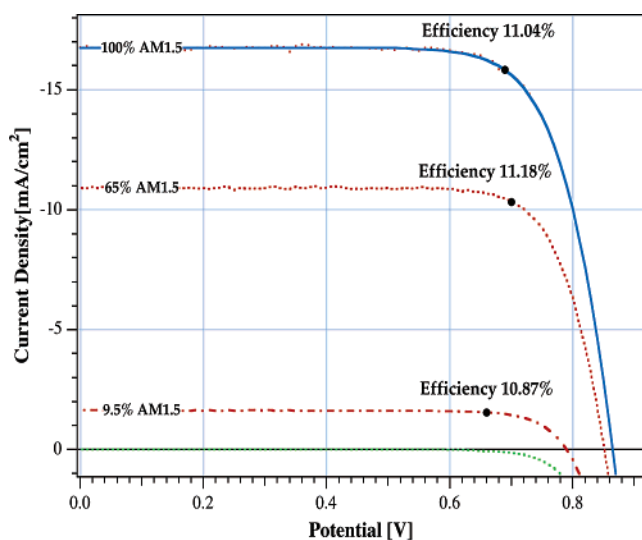


Figure 15. Photocurrent–voltage curve of a DSC at different light intensities. The conversion efficiency in full AM 1.5 sunlight was 11.04%. It increased to 11.18% at 65% full sunlight.

A heat-resistant quasi-solid-state electrolyte based on imidazolium iodide was introduced. When used in conjunction with the amphiphilic ruthenium dye Z-907, it was possible to pass for the first time the critical 1000-h stability test at 80 °C with a DSC.<sup>47</sup> Other laboratories have also presented systematic verifications of the cell stability carried out independently.

Very recently, heteroleptic ruthenium complexes such as the K-19 dye have been introduced, which because of the extension of  $\pi$  conjugation on one of the bipyridyl ligands shows enhanced light absorption in the visible.<sup>48</sup> Excellent

(44) Bach, U.; Tachibana, Y.; Moser, J.-E.; Haque, S. A.; Durrant, J. R.; Grätzel, M.; Klug, D. R. *J. Am. Chem. Soc.* **1999**, *121* (32), 7445.

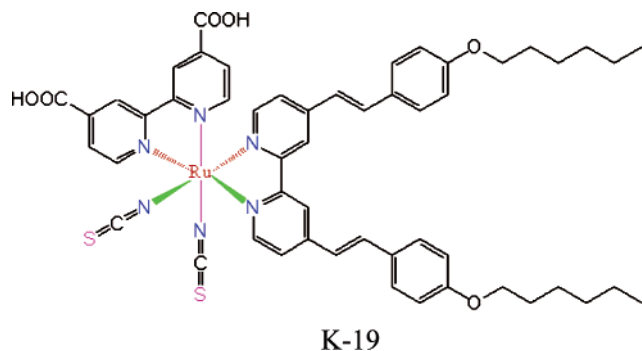
(45) Dloczik, L.; Ieperuma, O.; Lauermaun, I.; Peter, L. M.; Ponomarev, E. A.; Redmond, G.; Shaw, N. J.; Uhlendorf, I. *J. Phys. Chem. B* **1997**, *101*, 10281.

(46) Hinsch, A.; Kroon, J. M.; Kern, R.; Uhlendorf, I.; Holzbock, J.; Meyer, A.; Ferber, J. *Prog. Photovoltaics* **2001**, *9*, 425.

(47) Wang, P.; Zakeeruddin, S. M.; Moser, J. E.; Nazeeruddin, M. K.; Sekiguchi, T.; Grätzel, M. *Nat. Mater.* **2003**, *2*, 402.

(48) Wang, P.; Klein, C.; Humphry-Baker, R.; Zakeeruddin, S. M.; Grätzel, M. *J. Am. Chem. Soc.* **2005**, *127*, 808.

stability results under both long-term heat stress and light soaking have been obtained with these sensitizers.<sup>49</sup>



The use of solvent-free electrolytes such as ionic liquids has made striking advances during the past few years.<sup>37,50</sup> These nonvolatile redox melts show great promise for use in outdoor photovoltaic systems and have been discussed in detail elsewhere.<sup>51</sup>

(49) Wang, P.; Klein, C.; Humphry-Baker, R.; Zakeeruddin, S. M.; Grätzel, M. *Appl. Phys. Lett.* **2005**, *86*, 123508.

(50) Kato, T.; Okazaki, A.; Hayase, S. *Chem. Commun.* **2005**, 363.

### First Large-Scale Field Tests and Commercial Developments

During recent years, industrial interest in the DSC has surged and the first commercial products have appeared. A number of industrial corporations, such as Konarka ([www.konarkatech.com](http://www.konarkatech.com)) in the U.S.A., Aisin Seiki in Japan, RWE in Germany, and Solaronix in Switzerland, are actively pursuing the development of new products. Particularly interesting are applications in building integrated photovoltaic elements such as electric-power-producing glass tiles. The Australian company Sustainable Technologies International ([www.sta.com.au](http://www.sta.com.au)) has produced such tiles on a large scale for field testing and the first building has been equipped with a wall of this type.

**Acknowledgment.** Recognition is due to the members of the EPFL electrochemical photovoltaics development team, some of whose work is referenced below, and to those industrial and public organizations whose interest in this new system has induced them to support our research.

IC0508371

(51) Grätzel, M. *Photochem. Photobiol. A* **2004**, *164*, 3.